

Experimental and Numerical Performance Survey of a MW-Scale Supercritical CO₂ Compressor Operating in Near-Critical Conditions

Lorenzo Toni
Team Leader - Aerodynamics
Baker Hughes
Firenze, Italy

Giacomo Persico
Associate Professor
Politecnico di Milano
Milano, Italy

Ernani Fulvio Bellobuono
Senior Engineer - Aerodynamics
Baker Hughes
Firenze, Italy

Alessandro Romei
Research Fellow
Politecnico di Milano
Milano, Italy

Roberto Valente
Senior Engineer - Aerodynamics
Baker Hughes
Firenze, Italy

Paolo Gaetani
Professor
Politecnico di Milano
Milano, Italy



Lorenzo Toni is Team Leader for aerodynamic design within centrifugal compressors and turbo-expanders new product development department at Baker Hughes. His responsibilities include the centrifugal compressors aerodynamic design, aeromechanic modelling and analysis and performance predictability. Prior the current role he has been Senior Engineer for aerodynamics and Test and Data Analysis Engineer in GE Oil & Gas. He received an M.S. degree in Mechanical Engineering from the Florence University in 2005 and earned a PhD in Energetics from the same University in 2009. He is the author of several technical papers and patents in the field of turbomachinery.



Ernani Fulvio Bellobuono is a Senior engineer in the New Product Development team in Baker Hughes, where he works on aerodynamic design for advanced compression systems with main regards to LNG and energy transition products. As background Ernani holds a PhD in Aerospace Engineering from University of Naples and a post graduate Master in Management & Economics of Energy Firms from ENI Corporate University.



Roberto Valente is a Senior Aerodynamics Engineer for New Product Development group at Baker Hughes. He received a M.S. degree in Mechanical Engineering from the University of L'Aquila in 2005 and earned a PhD in Mechanical Engineering from the same University in 2009. He joined Baker Hughes in 2011 as Centrifugal Pumps Lead Design Engineer within the New Product Introduction team and then moved to his present position in 2014. His current responsibility is the aerodynamic design of centrifugal compressor stages.



Giacomo Persico is Associate Professor at Politecnico di Milano, Italy. He graduated in Mechanical Engineering in 2002 and earned a Ph.D. title in Energy in 2006. He was visiting researcher at the Von Karman Institute for Fluid Dynamics in 2005-2006 and visiting Professor at Saint Petersburg Polytechnical University in 2016-2018. His main research interests are unsteady flows, design and optimization methods, sCO₂ and ORC power systems, wind turbines. Prof. Giacomo Persico is author of more than 130 publications appearing in international Journals or Conference Proceedings. Two papers presented at the ASME Turbo Expo 2019 received the ASME IGTI Best Paper Award by the supercritical CO₂ power cycle and wind energy committees.



Alessandro Romei is a research fellow at Politecnico di Milano, where he also earned his Ph.D. in 2021. He was visiting researcher at the Von Karman Institute for Fluid Dynamics in 2016 and at the Ecole Polytechnique in 2019. His main research interests are shape optimization and uncertainty quantification technique applied to expansive simulations and design of turbomachinery operating in the non-ideal compressible fluid dynamic regime, such as turbines for organic Rankine cycles and compressors for supercritical carbon dioxide applications. Alessandro Romei is the author of about 15 papers presented at international conferences or published in peer-reviewed journals. His paper presented at the ASME Turbo Expo 2019 received one of the ASME IGTI Best Paper Awards by the supercritical CO₂ power cycle committee. He was also awarded the ASME IGTI Student Advisory Committee Travel Award in 2020 and 2021.



Paolo Gaetani is currently Full Professor of Turbomachinery at Politecnico di Milano, where he also took his Master degree in Mechanical Eng. and his PhD in Energetics.

His main research activities are in the unsteady aerodynamic of turbomachinery, mainly in the experimental field, focusing on stator – rotor and combustor-turbine interaction. He's been contributing to develop high promptness aerodynamic probes and miniaturised thermocouple. He's also actively working on the design of turbomachinery both turbine and compressors with specific focus on non-conventional fluids like ORC and sCO₂.

ABSTRACT

Closed power cycles based on carbon dioxide in supercritical conditions (sCO₂ in the following) are experiencing a growing scientific, technical and industrial interest, due to the high energy conversion efficiency and components compactness. Despite these advantages, the use of a working fluid operating in proximity to the critical point, especially for the compressor, entails multidisciplinary challenges related to the severe non-ideality of the supercritical fluid, which includes the potential onset of phase change at the impeller intake. On the technical and industrial grounds, the phase-transition might dramatically affect the aerodynamics, the performance and the rangeability of the compressor. On the scientific ground, the modelling of two-phase flows in transonic/supersonic conditions still remains an open issue that demands a thorough experimental assessment.

This work illustrates the results of a wide experimental campaign focused on the evaluation of the operative map of a MW-scale high-load sCO₂ compressor operating in plant-representative

conditions, i.e. in proximity to the critical point ($P = 79.8$ bar, $T = 33^\circ\text{C}$), designed in the frame of the sCO₂Flex project, EU Horizon 2020 funded program (grant agreement #764690). In the design process, the machine had been object of a thorough computational investigation, performed by using a homogeneous equilibrium model equipped with a barotropic equation of state, which revealed a significant impact of the phase change on the compressor aerodynamics and on its rangeability for flow rates higher than the design one. Such phenomena are connected to the sudden drop of the speed of sound, originated when the fluid thermodynamic condition crosses the saturation line, and they weaken as the compressor loading reduces. Experiments carried out on a first of a kind 5 MW sCO₂ prototype compressor manufactured and tested by Baker Hughes in 2021 remarkably well matched the predicted compressor performance and, especially, the anticipated and sudden choking of the compressor at nominal peripheral Mach number.

Results demonstrates experimentally, for the first time ever, the effects of the phase-change on the operation of a realistic sCO₂ compressor, also providing significant insights on the predictive capabilities of the physical models employed for the calculation of two-phase flows in this class of machines.

INTRODUCTION

Carbon dioxide in supercritical thermodynamic state is a favourable working fluid for energy systems from several perspectives. It exhibits low toxicity and thermal stability for very wide ranges of pressure and temperature, and used in closed Joule-Brayton cycles it offers potential advantages in terms of cycle efficiency and components size. For the reasons above reported, it is suited for operating in flexible environment (such as in combination to renewable sources and waste heat recovery). Besides the high thermal efficiencies by using sCO₂ as a working fluid, there is also the advantage of a simple and compact physical footprint coupled with a good operational flexibility, which could realize potential benefit also for Floating Production Storage and Offloading (FPSO) applications. These sCO₂ power systems are characterized by a compressor operating close to the critical point, typically featuring lower entropy with respect to the critical one so to minimize the compression work. Feasibility studies [1] suggest that for cycle power capacities within 300 MW the recommended machine is a centrifugal compressor. Typical pressure ratios of optimized sCO₂ power systems are of the order of 3 [2], which can be delivered by using either a single-stage or a two-stage compressor, anyway featuring high aerodynamic load in both cases.

The design and operation of high-speed turbomachinery in proximity to the critical point pose important scientific and technical challenges whose proper mastering is instrumental for the success of the entire sCO₂ technology. Close to the critical point, the large gradients in density and specific-heats make his behaviour deviate from the ideal-gas law [3] and, due to the proximity to the saturation curve, phase-change phenomena can also take place as a consequence of the local flow accelerations. The phase change can occur either as cavitation or condensation, depending on the entropy level of the CO₂ at the compressor intake, with important potential implications in terms of performance, rangeability and mechanical integrity. Criteria for avoiding two-phase flows were proposed [4] which end up in severe limitations in the selection and design of the compressor, especially when considering the high aerodynamic loading expected for this class of machines (unless several compression stages are considered).

Due to the low time-scale of the flow processes within compressor impellers, one potential advantage in the sCO₂ compressor operation might be the existence of meta-stable states, which results in a delay in the phase-change phenomena similar to that observed in wet steam

turbines [5], and already observed experimentally for condensing sCO₂ in nozzles [6]. However, similar experiments for flashing sCO₂ in nozzles [7] did not exhibit a delay in phase change (it is to be considered that the thermodynamic region where meta-stable states can exist becomes progressively thinner approaching the critical point).

In this uncertain scenario, it is crucial to develop appropriate models for the prediction of sCO₂ compressor aerodynamics with high fidelity from the thermodynamic perspective. Moreover, there is a clear need of reliable experimental data, performed considering real-scale machines operating in their actual condition and experiencing a realistic aerodynamic loading. As a relevant example, experimental [8] and computational [9, 10] studies were successfully performed on the compressor designed and operated at the Sandia Lab; however, the available experimental data considered a small-scale prototype operated with a limited pressure rise, so the machine was found to be virtually free from any significant two-phase flow effect. Other experimental studies on exemplary sCO₂ compressors have been recently presented [11], but again selecting thermodynamic states and aerodynamic loading to avoid two-phase flows. The experimental campaign presented in [12] and [13] deals with the design and development challenges faced on a 2.5MW sCO₂ compressor focusing rotordynamics and flow range. Performance measurements have been carried out on the same machine [14], whose suction pressure is closer to critical point than aforementioned cases, though with higher margin to saturation with respect to present work. On numerical side [15] the impact of inlet conditions when operating close to critical point has been assessed, but no experimental validation is available.

A gap exists, therefore, for the proper characterization of the sCO₂ compressors in presence of two phase flow conditions.

This work aims at filling this gap by presenting a unique set of experimental data and computational predictions performed on a MW-scale centrifugal compressor, designed in the frame of the EU-H2020 project sCO₂-Flex, featuring thermodynamic and operative conditions representative of those expected in the actual engineering application. sCO₂-Flex proposes a new closed-loop thermodynamic cycle to improve the flexibility and efficiency of existing conventional power plants while minimizing water usage. The system includes an axial expander and two centrifugal compressors working in parallel, and it is designed to provide 25 MWe at 100% load and have the flexibility to reduce load down to 20%; compared to a water/steam plant, sCO₂-flex can reduce greenhouse gases emissions by 8%. Baker-Hughes was in charge of performing the plant simulation for both design and off-design conditions, of selecting materials and perform relevant tests, of designing the two compressors and the expander and moreover of testing the prototype compressor working close to CO₂ critical point.

Beside the data, the paper discusses methodologic aspects related to both instrumental and numerical issues. By virtue of the good agreement between experiments and simulations, important conclusions will be drawn on physical aspects of the flow and their proper modelling.

COMPUTATIONAL MODEL

The CFD simulations presented in this paper were performed by applying the computational flow model developed by the Politecnico di Milano for the high-fidelity analysis of compressible flows in turbomachinery operating with non-ideal working fluids. The flow model is based on the ANSYS-CFX finite-volume flow solver, using high-order numerical schemes for both inviscid and viscous fluxes. Turbulence effects are introduced by resorting to the $k-\omega$ SST model [16] assuming fully turbulent flow. Considering the very low kinematic viscosity of carbon dioxide in supercritical conditions, the assumption of hydraulically smooth surfaces is not appropriate and, hence, wall roughness and wall functions are specified.

Even though based on a RANS level of approximation, the high-fidelity of the present model refers to the accurate representation of the thermodynamic behaviour of the fluid. This is crucial for the proper modelling of turbomachinery operating with fluids in supercritical conditions, whereby the proximity to the critical points originates a large departure from ideal-gas behaviour. In particular, the thermodynamic behaviour of the fluid is modelled here by resorting to the Span-Wagner formulation [17]. However, the challenges of simulating the flow in technically-relevant sCO₂ compressors are also related to two-phase flows: the proximity of the inlet compressor state to saturation might indeed trigger phase change processes that need to be taken into account in the simulation model. In this work, we make use of a barotropic model, which belongs to the class of homogeneous equilibrium models (HEM); the barotropic model was first proposed for application to sCO₂ compressors by the same authors in [18], and it was subsequently discussed and compared against a non-barotropic HEM in [19]. The barotropic model provided computational results in excellent validation against experiments for flashing expansions of sCO₂ [7], in particular for thermodynamic states close to the ones of interest for the present case and sCO₂ compressors in general.

The equations of motion are solved on structured meshes composed by hexahedral elements. Meshes are generated applying AutoGrid™ and include the intake duct, the impeller, with fillet radii, and the vaneless diffuser. The leaks in the seals and the related secondary flows were not the object of the CFD simulation and, hence, not modelled.

PROTOTYPE COMPRESSOR AND RIG LAYOUT

Prototype compressor is a 2 stages centrifugal compressor with an operating range between 60% and 105% speed; a barrel type casing has been chosen taking into account the operating pressure. Rotor is composed by the shaft and two impellers: the first one has a dedicated design to cope with the CO₂ supercritical characteristics, in proximity of critical point, whereas the second one belongs to Baker Hughes centrifugal compressor stages database. Figure 1 shows the barrel compressor casing and a schematic cross section of the compressor itself.

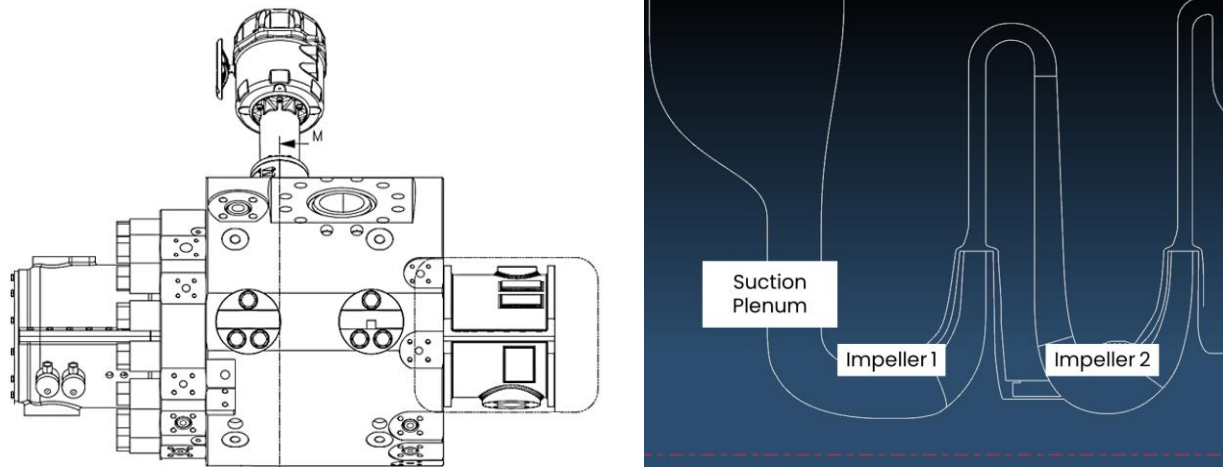


Figure 1 – Barrel Compressor Casing (left) and schematic cross section (right)

Test has been carried out on a test bench in the Baker Hughes facility in Florence, see Figure 2, which allowed for testing the 5.4 MW compressor prototype and exploring the whole operating map. Test was performed in a closed loop and a gas turbine was used as a driver. Figure 3 depicts the compressor installed on the test rig.

Dealing with supercritical CO₂ has been the main challenge of the design of prototype and test facility. Due to the already described peculiarity of the compressor suction conditions and the strict tolerances required, particular care was given to temperature control, in order to avoid uncontrolled phase transitions in all tested operating conditions, both steady state and transient.

The test was an ASME PTC-10 Type I test, hence executed under conditions equal to the design ones (e.g., gas composition and inlet total temperature and pressure): the final goal was to measure the compressor performances. Instrumentation was selected to achieve the highest level of accuracy in performance and controllability; moreover, additional internal compressor measurements were added to address detailed verification of machine components. In particular, since the first stage is the one having suction conditions close to the critical point, static pressure taps have been placed at impeller inlet and along the diffuser; at the same time total pressure and total temperature probes have been installed at the inlet and outlet of the first stage diffuser. In addition, compressor flowrate was measured both at compressor suction and discharge.

The accuracy of both temperature and pressure measurements plays a major role in performance computation; for this reason special care is needed when sensors and instrumentation are selected. As far as temperature measurements are concerned, RTD (resistance temperature detector) class A+ were selected and they were calibrated with a primary source, returning an uncertainty of ± 0.04 K. The instrumentation uncertainty for total pressure measurements is reported in table below, for two relevant conditions (see also next chapter): far from critical point operation (50 bar, 309.15 K at compressor inlet) and design point operation (79.79 bar, 306.15 K). Since all the sensors and transducers ranges were identified to guarantee better performance when operating in design conditions (hence close to critical point) the uncertainty levels in the far from critical point conditions (where absolute pressure levels both at the inlet and at the outlet are lower) are slightly higher.

	<i>Far from Critical Point</i>	<i>Design Operation</i>
P_{in}	0.13%	0.07%
P_{out}	0.28%	0.08%

Table 1 – Total Pressure Measurement Uncertainty

The mass flow rate was measured using orifice plates, according to ASME 5167 standard, with a relative uncertainty in the order of 0.8%. The relative uncertainty in rotational speed is below 0.01%.

Regarding the main performance parameters, table below collects the measurement uncertainty. As shown, in both cases the measurement uncertainty, which takes into account both sensors/transducers accuracy and signals standard deviation during test points acquisition, is considered very good and in line with industrial expectations. Due to lower measurement uncertainty in the design condition, the uncertainty on performance keeps lower as well.

	<i>Far from Critical Point</i>	<i>Design Operation</i>
Flow Coefficient	1.32%	0.86%
Polytropic Efficiency	2.37%	1.82%
Pressure Ratio (Total-Total)	0.31%	0.11%

Table 2 – Uncertainty on Performance



Figure 2 – Prototype compressor test rig at the Baker Hughes facility in Florence, Italy



Figure 3 – Prototype installed on the test rig at the Baker Hughes facility in Florence, Italy

RESULTS AND DISCUSSION

The final goal of experimental test campaign was the performance measurement of the compressor operating in plant-representative conditions, i.e. in proximity to the critical point (CP), at $P = 79.8$ bar and $T = 33^\circ\text{C}$. Moreover, in order to carry out an in depth assessment of the thermodynamic behavior and performance of a compressor operating in such peculiar conditions, a first test campaign was focused on the performance measurements in a far from critical point condition. Table 3 collects the main operating parameters for the two conditions, which are then graphically represented on P-S diagram in Figure 4

	<i>Far from Critical Point</i>	<i>Design Operation</i>
Gas	CO_2 (100%)	CO_2 (100%)
Suction Total Pressure	50.0 bar	79.79 bar
Suction Total Pressure	309.15 K	306.15 K
Shaft Speed	8625 rpm	11400 rpm

Table 3 – Operating Conditions

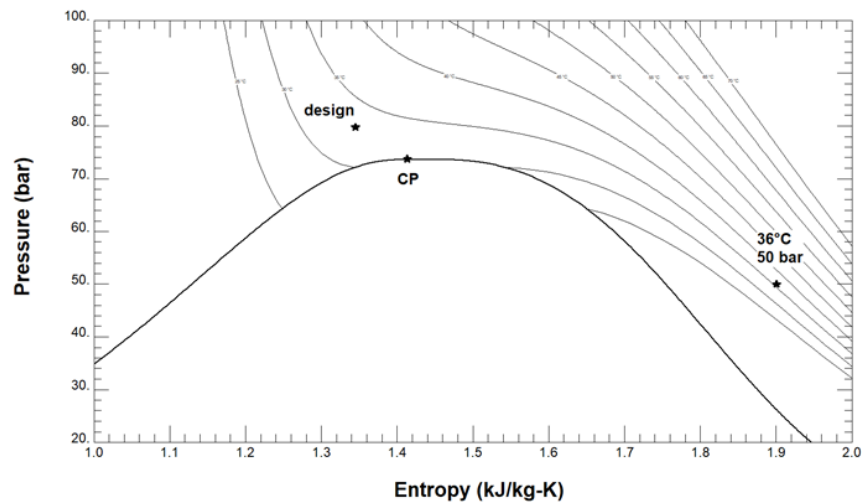


Figure 4 – Inlet conditions on P-S state diagram for performance far from critical point

Both in the design condition and in the one far from critical point, a complete curve exploration from the right to the left flow rate limit was performed.

Due to the peculiar suction conditions for design point case, in particular to the proximity to CO₂ critical point, it has been very important to guarantee inlet conditions close to design values all along the performance curve and to guarantee full stable conditions. At this regards a line-up of deviations for the design curve is shown in Figure 5 where, in the range tested, deviations for suction temperature and pressure are in the range of ±1%.

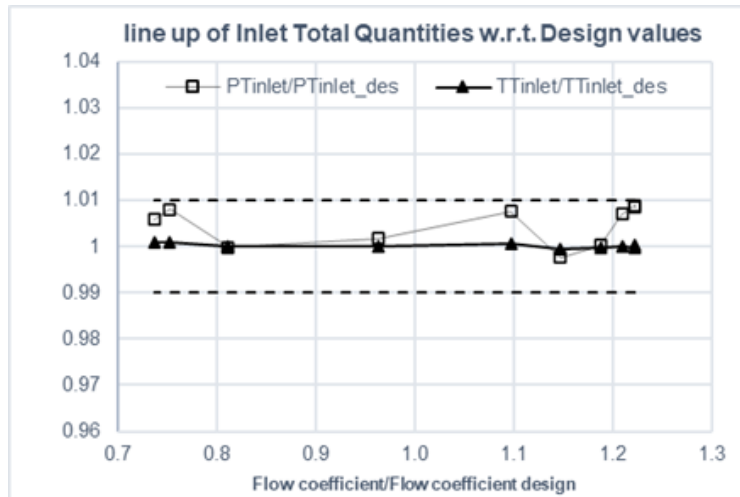


Figure 5 – Variation of inlet pressure and temperature during exploration of 100% speed curve

Far from Critical Point Performance

In the first part of the test campaign, the machine was operated far from critical point (see again Figure 4) where thermodynamic quantities are characterized by properties well approximated by the ideal gas model. Test results are given in Figure 6, where flow coefficient, total pressure ratio and efficiency are defined as:

$$\phi = \frac{4Q}{\pi D_2^2 u_2} \quad \text{Equation 1}$$

$$\beta_{FF} = \frac{P_{tot,2}}{P_{tot,1}} \quad \text{Equation 2}$$

$$\eta_{FF} = \frac{\Delta h_{pol}}{\Delta h_{ad}} \quad \text{Equation 3}$$

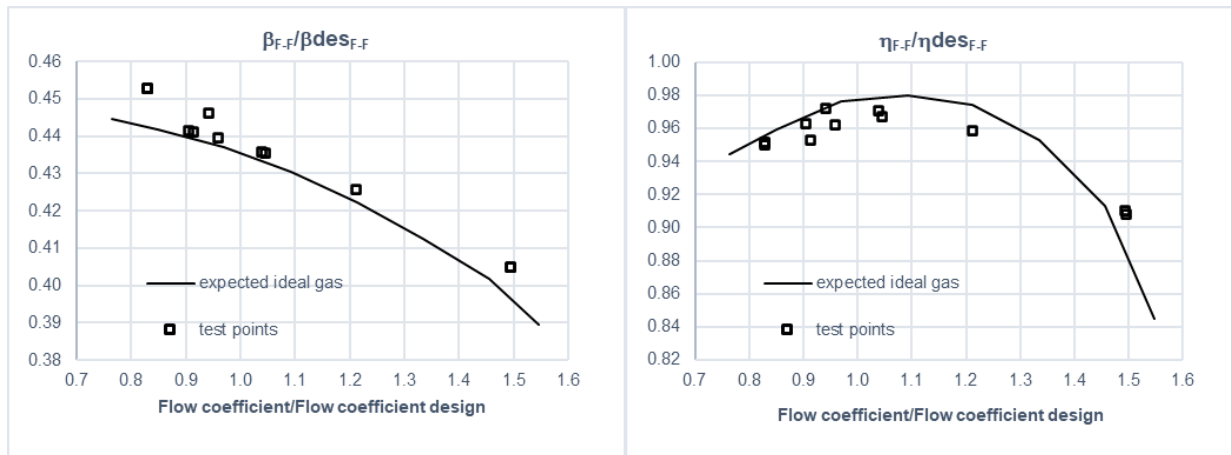


Figure 6 – Performance curves far from critical point

Results are in good agreement with experimental data. Two points in left region of β_{FF} plot of Figure 6 appear out of trend with respect to rest of the curve: indeed those two points have been obtained with same inlet condition but with a slightly higher speed (thus, with a slightly higher peripheral Mach number) that led to a higher pressure ratio as well. Such points have been kept anyway in the experimental set of data as they are useful to better describe left region.

Obtained results confirm that in these conditions, where inlet pressure and temperature are very far from CP, the assumption of considering ideal gas properties is a proper choice to predict performance. On the contrary, as it will be shown in the following section, the assumption of ideal gas for inlet conditions close to CP leads to a not-acceptable over estimation of the right flow rate range limit.

Design Point performance

In this work, only results obtained at nominal rotational speed are discussed. The experimental curves in terms of pressure ratio and normalized total-to-total efficiency are reported in Figure 7 and compared with two sets of expected curves obtained via CFD simulations. As their name suggest, the “*ideal-gas expected*” curves are obtained under the ideal-gas approximation with constant specific heat coefficients, while the so-called “*real-gas expected*” curves are derived by accounting for the actual volumetric evolution as predicted by the barotropic method..

For $\phi/\phi_a < 1.2$, the two numerical curves, normalized by their design values, overlap and reproduce the experimental data with an acceptable approximation. A first qualitative difference can be found in the slope of pressure rise, which is slightly underpredicted by the expected curves. However, this discrepancy does not undermine the compressor stability, which was preserved even for $\phi/\phi_a < 0.8$. Instead, the shape of the efficiency curve is closely reproduced for these flow conditions, with a uniform overprediction of few percentage points. It is worth to underline that a similar relative error is also found for conditions far from the critical point (see Figure 6), whereby the measurement uncertainty is also comparably lower.

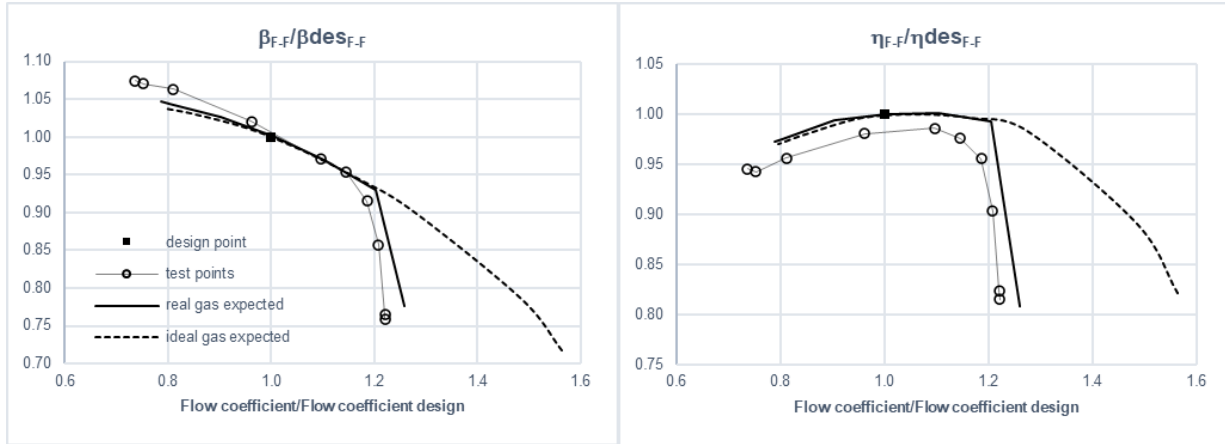


Figure 7 – 100% speed - comparison with expected

The two expected curves depart for $\phi/\phi_d > 1.20$. The *real-gas expected* exhibits a sharp drop in performance connected to choked operation that is coherent with experimental data, while the *ideal-gas expected* reaches $\phi/\phi_d = 1.55$. The flow fields in terms of relative Mach number at three relevant spanwise coordinate obtained with both the ideal gas and barotropic model are reported in Figure 8 for $\phi/\phi_d = 1.20$. A sonic throat at the hub section (10% of the span) confirms that the barotropic model predicts choke in this flow condition, opposed to the ideal-gas scenario, in which $M_w \approx 0.5$. The earlier onset of a sonic throat cannot be explained by simply resorting to conventional single-phase thermodynamics: the speed of sound generally decreases with fluid compressibility, then a perfect gas should exhibit a higher Mach number than its real-gas counterpart (featuring lower compressibility). Therefore, the responsibility for a reduced choking limit should be found elsewhere, e.g. in the onset of the phase change.

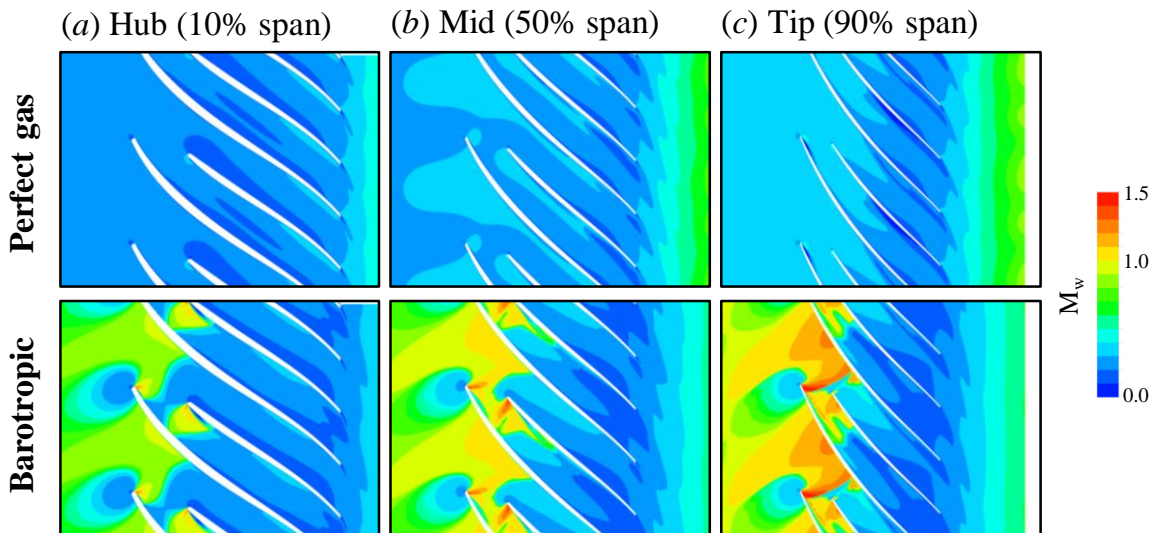


Figure 8 – Comparison of relative Mach number fields obtained with the perfect-gas (top panels) and barotropic (bottom panels) model for three spanwise sections, namely (a) hub (10% span), (b) mid (50% span), and (c) tip (90% span) at $\phi/\phi_d=1.20$.

The two-phase states computed with the barotropic model follow the thermodynamic equilibrium. From a physical perspective, this assumption is justified because non-equilibrium drivers - such as surface tension, latent heat, density ratio between phases, metastable states - vanish approaching the critical point. Under this assumption, a significant drop in the speed of sound (more than halved) is observed when crossing the saturation curve. Therefore, the sudden increase in Mach number is not prompted by an appreciable variation of the flow velocity, but instead by a reduction of the speed of sound connected with the onset of the secondary phase (lighter than the primary phase). To this end, Figure 9 shows the flow fields of speed of sound and relative Mach number for three flow conditions, namely a low flow rate (close to surge), design flow rate and high flow rate (choked flow rate). By comparing the two fields, it is evident that the Mach number increase is largely triggered by the drop in the speed of sound associated with the onset of the two-phase flow, explaining the early choking that is experimentally observed. This strong experimental evidence supports that *two-phase flows occurring close to the critical point quickly achieves the thermodynamic equilibrium*, and non-equilibrium or metastable effects play a marginal role.

From an operation viewpoint and for the design operating condition here documented, no specific shaft vibration frequencies associated with the onset of two-phase flows were detected during the test campaign. An explanation can be found in the relatively small density ratio between the liquid and vapor phase (less than one order of magnitude). Therefore, the secondary phase is expected to be dispersed into the primary one without a clear phase interface (bubbly flow regime), thus possibly weakening the two-phase flow dynamics.

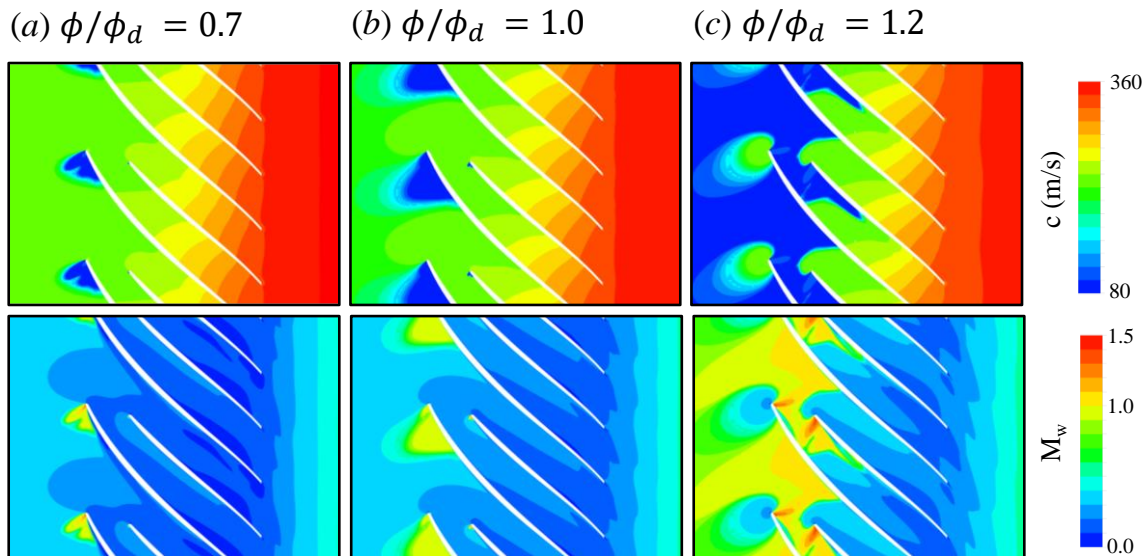


Figure 9 – Midspan flow fields in terms of speed of sound (top panels) and relative Mach numbers (bottom panels) for three representative flow conditions, namely a (a) low flow rate, (b) design flow rate, and (c) choking flow rate.

To better highlight phase-change processes, Figure 9 reports the iso-surfaces of saturation pressure for surge, design and choked flow conditions. For this latter, the enclosed volume delimited by the iso-surface is expected to be single-phase, opposed to the first two cases, in which the two-phase is enclosed by the iso-surface. For $\phi/\phi_d = 1.20$, the total-to-static expansion responsible of the flow rate is sufficient to trigger phase transition, thus the flow is entirely two-

phase at the impeller entrance. The single-phase condition is recovered in a local region close to the stagnation point, where the kinetic head vanishes and, accordingly, the static pressure rises (above the saturation one). For lower flow rates, instead, the flow is single phase at the entrance, but it becomes two-phase due to local flow acceleration on the main-blade suction side. Interestingly, a small two-phase flow region is found even at low flow rates $\phi/\phi_d = 0.70 - 0.80$ due to local flow acceleration, but no specific operational instabilities at low flow rate seemed to appear in the experiments. However, a clear analysis of the surge was not object of this experimental campaign, and further analyses are needed to corroborate this experimental evidence.

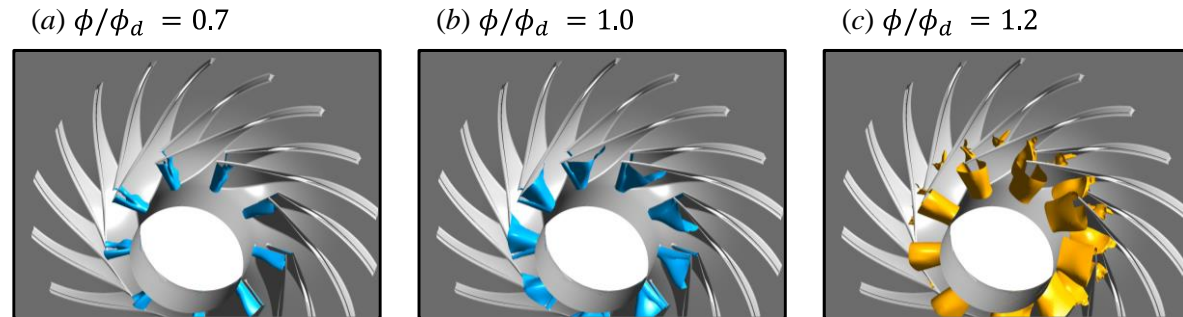


Figure 10 – Isosurfaces of saturation pressure for three representative flow conditions, namely a (a) low flow rate, (b) design flow rate, and (c) choking flow rate. The blue isosurface indicates that the corresponding enclosed region includes thermodynamic states such that $P < P_{sat}$, the opposite for the orange isosurface.

CONCLUSIONS

This work has presented a unique set of experimental data describing the operation of a MW-scale compressor working with sCO₂ in thermodynamic and load conditions representative of those expected in the actual engineering application. This is likely the first time a compressor of this size has been tested with CO₂ in supercritical conditions and it fulfilled all the aerothermodynamic requirements. As a relevant consequence, such tests have given the opportunity to assess the innovative computational model introduced within the sCO₂-flex project, which was shown to provide accurate performance predictions for centrifugal compressors working close to the CO₂ critical point. The matching between experiments and simulation has demonstrated that using sCO₂ as working fluid has an impact on the rangeability of the compressor, with an anticipation of the choking limit. This finding, suggested by previous studies of the same authors and fully confirmed by the present experiments, has been explained as a consequence of the onset of two-phase flows in the intake region of the machine. By confirming the numerical predictions, the experiments have also demonstrated that two-phase flow simulations based on the barotropic homogeneous equilibrium model are able to capture the effect of two-phase flows on sCO₂ compressor performance and rangeability.

This is deemed a milestone for the validation not only of sCO₂ turbomachinery but for the whole sCO₂ technology, bringing key learnings in terms of efficiency, manufacturability, and controllability, as well as on high-fidelity modelling, of one of its crucial components, the main compressor. The sCO₂-flex experience has enabled us to design turbomachinery to operate with supercritical CO₂ for selection and production of the most efficient, flexible, and cost-effective supercritical CO₂ cycles to help drive the energy transition.

ACKNOWLEDGEMENTS

This work was supported by the sCO₂-flex project, funded from the European Union's Horizon 2020 research and innovation programme under grant agreement N° 764690.

The authors would like to express their gratitude to Baker Hughes for providing the permission to proceed with publication and to Massimo Camatti for supporting this activity.

Thanks are due to Silvia Evangelisti, Giuseppe Nasca and Stefano Vanghi from Baker Hughes' Turbomachinery Testing Laboratory (TTL).

NOMENCLATURE

sCO ₂	Supercritical Carbon Dioxide
CFD	Computational Fluid Dynamics
CP	Critical Point
MW	Mega Watt
c	Speed of Sound
D	Diameter
h	Enthalpy
M	Mach number
P	Pressure
Q	Volumetric flow rate
S	Entropy
T	Temperature
u	Peripheral speed

Greeks

β	Pressure Ratio
φ	Flow coefficient
η	Polytropic efficiency
ρ	Density

Subscripts

ad	Adiabatic
d	Design
in	Compressor inlet flange
FF	Flange to Flange
out	Compressor outlet flange
pol	Polytropic
sat	Saturation
w	Relative quantity
2	Impeller trailing edge section

BIBLIOGRAPHY

- 1 K. Brun, P. Friedman and R. Dennis, Fundamentals and Applications of Supercritical Carbon Dioxide (sCO₂) Based Power Cycles, Woodhead Publishing, 2017.
2. A. Romei, P. Gaetani, A. Giotri and G. Persico, "The role of turbomachinery performance in the optimization of supercritical carbon dioxide power systems," Journal of Turbomachinery, vol. 142, no. 7, p. 071001, 2020.
3. N. D. Baldadjiev, C. Lettieri and Z. S. Spakovszky, "An investigation of real gas effects in supercritical CO₂ centrifugal compressors," Journal of Turbomachinery, vol. 137, no. 9, p. 091003, 2015.
4. T. C. Allison and A. McClung, "Limiting Inlet Conditions for Phase Change Avoidance in Supercritical CO₂ Compressors," in ASME Turbo Expo 2019: Turbomachinery Technical Conference and Exposition, Phoenix, Arizona, USA , 2019.
5. Moore, M J, and Sieverding, C H. Aerothermodynamics of low pressure steam turbines and condensers. United States: N. p., 1986.
6. C. Lettier, D. Paxson, Z. Spakovszky and P. Bryanston-Cross, "Characterization of nonequilibrium condensation of supercritical carbon dioxide in a de laval nozzle," Journal of Engineering for Gas Turbines and Power, vol. 140, no. 4, p. 041701, 2017.
7. M. Nakagawa, M.S. Berana and A. Kishine, "Supersonic two-phase flow of CO₂ through converging-diverging nozzles for the ejector refrigeration cycle", Int. J. Refrig. 32 (6) (2009) 1195–1202.
8. S. Wright, R. Radel, M. Vernon, G. Rochau and P. Pickard, "Operation and Analysis of a Supercritical CO₂ Brayton Cycle," SANDIA REPORT, SAND2010-0171, Albuquerque, New Mexico, 2010.
9. R. Pecnik, E. Rinaldi and P. Colonna, "Computational fluid dynamics of a radial compressor operating with supercritical CO₂," Journal of Engineering for Gas Turbines and Power, vol. 134, no. 12, p. 122301, 2012.
10. A. Hosangadi, Z. Liu, T. Weathers, V. Ahuja and J. Busby, "Modeling Multiphase Effects in CO₂ Compressors at Subcritical Inlet Conditions," Journal of Engineering for Gas Turbines and Power , vol. 141, no. 8, p. 081005, 2019.
- 11 S. K. Cho, S. Son, J. Lee, S-W. Lee, Y. Jeong, B. S. Oh and J. I. Lee, "Optimum loss models for performance prediction of supercritical CO₂ centrifugal compressor", Applied Thermal Engineering, Vol. 184, 2021, 116255.
12. S. Cich, J. Moore, C. Kulhanek and J. Mortzheim, "Development and Testing of a Supercritical CO₂ Compressor Operating Near the Dome", Turbomachinery and Pump Symposia, Texas A&M University, Houston, TX, September 15-17, 2020.
13. S. Cich, J. Moore, C. Kulhanek, M. Towler and J. Mortzheim, "Mechanical Design and Testing of a 2.5 MW SCO₂ Compressor Loop", ASME Turbo Expo, GT2021-04155, June 7-11, 2021.
14. J. Mortzheim, D. Hofer, S. Priebe, A. McClung, J. Moore and S. Chich, "Challenges with Measuring Supercritical CO₂ Compressor Performance When Approaching the Liquid Vapor Dome", ASME Turbo Expo, GT2021 59527, June 7-11, 2021.
15. R. Pelton and S. Jung, "Real gas effects on the off-design performance of a sCO₂ compressor", Proceedings of Global Power and Propulsion Society, GPPS-TC-2019-0087, January 16-17, 2019.

16. F. R. Menter, "Two-Equation Eddy-Viscosity Turbulence Models for Engineering Applications," *AIAA Journal*, vol. 32, no. 8, pp. 1598-1605, 1994.
17. R. Span and W. Wagner, "A New Equation of State for Carbon Dioxide Covering the Fluid Region from the Triple-Point Temperature to 1100 K at Pressures up to 800 MPa," *Journal of Physical and Chemical Reference Data*, vol. 25, no. 6, pp. 1509-1596, 1996.
18. G. Persico, P. Gaetani, A. Romei, L. Toni, E. Bellobuono and R. Valente, "Implications of phase change on the aerodynamics of centrifugal compressors for supercritical carbon dioxide applications", *J. Eng. Gas Turbines Power* 143 (4) (2021) 041007, <http://dx.doi.org/10.1115/1.4049924>.
19. A. Romei and G. Persico, "Computational fluid-dynamic modeling of two-phase compressible flows of carbon dioxide in supercritical conditions," *Applied Thermal Engineering.*, Vol. 190, 2021.